The distribution of stresses and strains in the mating elements disk tools working bodies of roadheaders

A A Khoreshok[1,a], L E Mametyev[2,b], A Yu Borisov[3,c], A V Vorobyev[4,d]

[1,2]Prof. dr.-ing., [3]head teacher, [4]candidate of science (engineering), associate professor
[1,2,3]Department of Mining Machines and Complexes/Mining Institute,
T.F. Gorbachev KuzSTU, Russia, 650000, Kemerovo, Vesennyaya street 28,
[1,4]Department of Mining Equipment, Yurga Institute of Technology, TPU affiliate
Russia, 652055, Yurga, Leningradskaya street 26
E-mail: [a] haa.omit@kuzstu.ru, [b,c] bau.asp@rambler.ru, [d] vorob@tpu.ru

Abstract. Presents the results of modeling the stress-strain state in the mating structural elements of the attachment disk tools various design on triangular and tetrahedral prisms working bodies of roadheaders selective action in the destruction of coalface of heterogeneous structure.

1. Introduction

In the world practice of conducting underground mining is a widespread tool, disc and roller tools to equip working bodies roadheaders, shield tunneling complexes and aggregates [1–13]. The Department Mining machines and complexes, T.F. Gorbachev KuzSTU together with the Department of Mining Equipment of YUTI (affiliate) TPU conducted research aimed at developing constructive modules of the attachment disk of the instrument, is in charge of maintaining the extension of the scope of working bodies of roadheaders selective action on the destruction of structurally heterogeneous coal and rock face. Evaluation of the effectiveness of the developed technical solutions is carried out by results of modeling the stress-strain state of the use of the finite element method.

2. The distribution of equivalent stresses in conjugate constructive elements of the attachment of the disk tool to a polygonal prisms

When modeling the stress state of structures of triangular prisms with the attachment of the three options (Figure 1, a, b, c) and tetrahedral prisms (Figure 1, d, e) used four design disk tool diameter D = 160 mm (three biconical with angles of taper: $1 - \varphi = \varphi_1 + \varphi_2 = 5° + 25° = 30°$; $2 - 10° + 20° = 30°$; $3 - 15° + 15° = 30°$ and one tapered $4 - \varphi = 0° + 30°$). It should be noted that the angle of taper φ_1 biconical disc facing tool to the surface of the exposed face of the tunnel excavation.

In table 1 and Figure 2 presents the dependence of the equivalent stress distribution σekv from conjugate diameters D of the structural elements of the attachment of the disk tool to the triangular prisms for the predicted coalface fracture of rocks with σcomp = 70 MPa. At the same characteristic cross sections pass through the edge of the disc and following cross mating elements: - for the first variant in Figure 1, a (1 – disc, 2 – axle-pivot), for the second and third variants in Figure 1, b (1 – disc, 2 – pivot, 3 – axle with thrust collar).
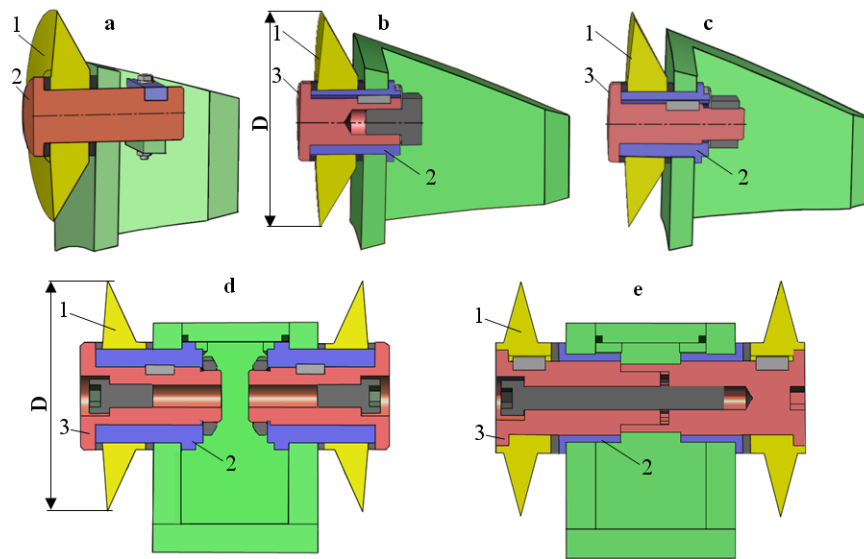
Figure 1. The design of the mating elements of the attachment of the disk tool on the polygonal prisms: a – with strap-lock, b – with screw; c – with nut; d – separated nodes mount disks; e – tandem nodes mount disks

Table 1. The distribution of equivalent stresses in the destruction of the face

disk tool on the triangular prism crowns roadheaders

| Options nodes attachment	The angles of taperdiscs $\varphi = \varphi_1 + \varphi_2, °$		Polynomial according	Validity coefficients of approximation R^2
I	1	5°+25°	$\sigma_{ekv} = -4E\text{-}10D^6 + 2E\text{-}07D^5 - 4E\text{-}05D^4 + 0.0036D^3 - 0.13D^2 + 2.1824D - 3.364$	0.9116
	2	10°+20°	$\sigma_{ekv} = -2E\text{-}10D^6 + 1E\text{-}07D^5 - 3E\text{-}05D^4 + 0.0028D^3 - 0.1138D^2 + 1.8771D - 2.6505$	0.9
	3	15°+15°	$\sigma_{ekv} = -4E\text{-}10D^6 + 2E\text{-}07D^5 - 5E\text{-}05D^4 + 0.0044D^3 - 0.1686D^2 + 2.5206D - 4.4542$	0.875
	4	0°+30°	$\sigma_{ekv} = 2E\text{-}10D^6 - 1E\text{-}07D^5 + 2E\text{-}05D^4 - 0.0011D^3 + 0.0297D^2 + 0.0692D + 0.8159$	0.8987
II	1	5°+25°	$\sigma_{экв} = -1E\text{-}10D^6 + 8E\text{-}08D^5 - 2E\text{-}05D^4 + 0.002D^3 - 0.0932D^2 + 1.8159D - 3.217$	0.9143
	2	10°+20°	$\sigma_{ekv} = 2E\text{-}10D^6 - 2E\text{-}08D^5 - 4E\text{-}06D^4 + 0.0011D^3 - 0.0686D^2 + 1.5676D - 2.8298$	0.8901
	3	15°+15°	$\sigma_{ekv} = 5E\text{-}10D^6 - 2E\text{-}07D^5 + 2E\text{-}05D^4 - 0.0008D^3 - 0.0002D^2 + 0.6508D - 1.3489$	0.8752
	4	0°+30°	$\sigma_{ekv} = 6E\text{-}10D^6 - 3E\text{-}07D^5 + 4E\text{-}05D^4 - 0.0031D^3 + 0.0984D^2 - 0.7694D + 2.4977$	0.9467
III	1	5°+25°	$\sigma_{ekv} = -1E\text{-}10D^6 + 6E\text{-}08D^5 - 1E\text{-}05D^4 + 0.0014D^3 - 0.0648D^2 + 1.5159D - 3.3668$	0.9004
	2	10°+20°	$\sigma_{ekv} = -3E\text{-}11D^6 + 6E\text{-}08D^5 - 2E\text{-}05D^4 + 0.0022D^3 - 0.1041D^2 + 2.0006D - 4.0917$	0.9003
	3	15°+15°	$\sigma_{ekv} = 4E\text{-}10D^6 - 1E\text{-}07D^5 + 1E\text{-}05\ D^4 - 4E\text{-}05D^3 - 0.0253D^2 + 0.921D - 1.7204$	0.9011
	4	0°+30°	$\sigma_{ekv} = -3E\text{-}10D^6 + 1E\text{-}07D^5 - 2E\text{-}05D^4 + 0.0012D^3 - 0.0291D^2 + 0.4971D + 0.2927$	0.8799
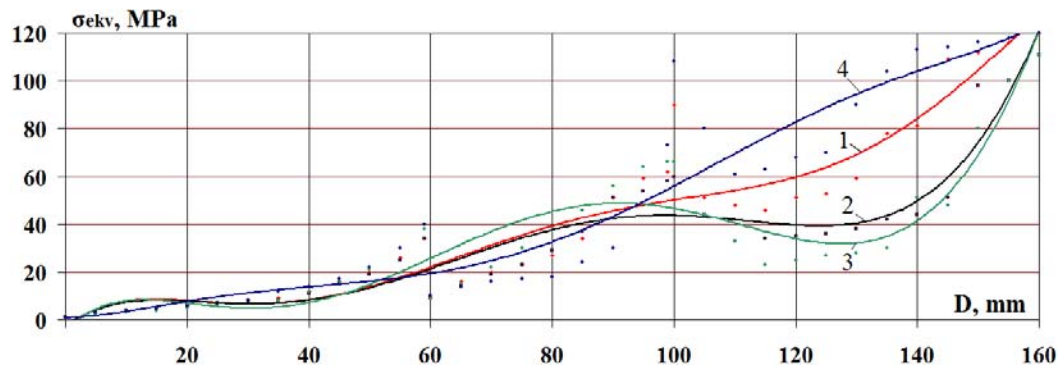
Figure 2. Dependence of the distribution of equivalent stresses σ_{ekv} of the diameter D of the mating structural elements in the cross section passing through the flange of the disk tool to a first variant of the attachment point to the triangular prism (Figure 1, a): 1, 2, 3, 4 – the angles of taper disks $\varphi = \varphi_1 + \varphi_2$ (table 1)

In table 2 and Figure 3, 4 shows the picture and dependence on the distribution of equivalent stresses σ_{ekv} from conjugate diameters D of the structural elements of the attachment with separate disk tools to a tetrahedral prism (Figure 1, d) for the predicted destruction of the face: coal (1 – σ_{comp} = 12.4 MPa), breed (2 – σ_{comp} = 51 MPa; 3 – σ_{comp} = 60.6 MPa; 4 – σ_{comp} = 78.9 MPa). Thus, the mating structural elements in the characteristic cross-section are (fig. 1, d): 1 – disc, 2 – pivot, 3 – axle with thrust collar.
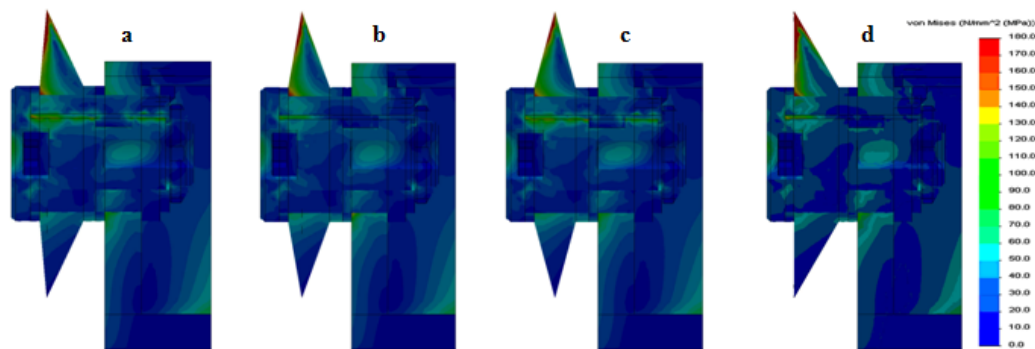

Figure 3. The distribution of equivalent stresses σ_{ekv} on the von Mises criterion in the attachment to the tetrahedral prism with the destruction of the rock mass σ_{comp} = 60.6 MPa separate disk tools with angles of taper: a – φ = 5°+25°, b – φ = 10°+20°; c – φ = 15°+15°; d – φ = 0°+30°
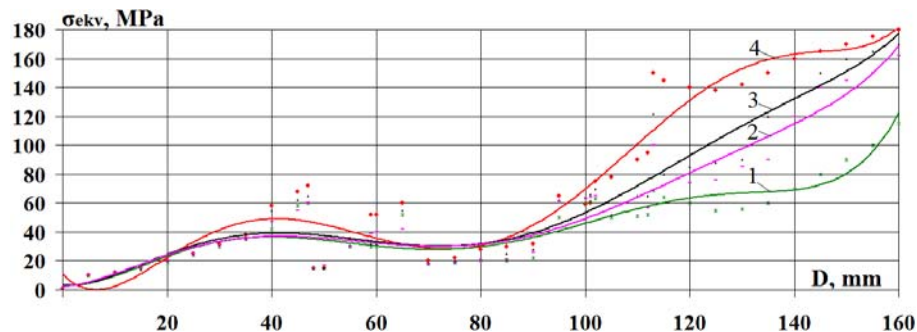

Figure 4. Dependence of the distribution of equivalent stresses σ_{ekv} of the diameter D of the mating structural elements in the cross section passing through the flange disk tool φ = 5°+25° attachment point to tetrahedral prism (table 2): 1 – σ_{comp} = 12.4 MPa; 2 – σ_{comp} = 51 MPa; 3 – σ_{comp} = 60.6 MPa; 4 – σ_{comp} = 78.9 MPa

Table 2. The distribution of equivalent stresses in the destruction of face
the separate disc tool on the tetrahedral prisms roadheaders

Corners sharpening two discs $\varphi = \varphi_1+\varphi_2,°$	Face σ_{comp}, MPa		Polynomial according	Validity coefficients of approximation R^2
5°+25°	1	12.4	$\sigma_{ekv} = 9E\text{-}10D^6\text{-}4E\text{-}07D^5+7E\text{-}05\ D^4-0.005D^3+0.1473D^2\text{-}0.4312D+3.5697$	0.8307
	2	51	$\sigma_{ekv} = 5E\text{-}10D^6\text{-}3E\text{-}07D^5+5E\text{-}05D^4-0.0034D^3+0.0955D^2+0.236D+2.227$	0.9124
	3	60.6	$\sigma_{ekv} = 6E\text{-}10D^6\text{-}3E\text{-}07D^5+5E\text{-}05D^4-0.0041D^3+0.1219D^2\text{-}0.0698D+2.6707$	0.9093
	4	78.9	$\sigma_{ekv} = 2E\text{-}09D^6\text{-}8E\text{-}07D^5+0.0001D^4-0.0115D^3+0.3972D^2\text{-}3.802D+11.028$	0.9305
10°+20°	1	12.4	$\sigma_{ekv} = 9E\text{-}10D^6\text{-}4E\text{-}07D^5+7E\text{-}05D^4-0.0051D^3+0.1618D^2\text{-}0.792D+4.5062$	0.8155
	2	51	$\sigma_{ekv} = 4E\text{-}10D^6\text{-}1E\text{-}07D^5+2E\text{-}05D^4-0.0011D^3\text{-}0.0011D^2+1.5566D\text{-}0.5273$	0.8962
	3	60.6	$\sigma_{ekv} = 7E\text{-}10D^6\text{-}3E\text{-}07D^5+5E\text{-}05D^4-0.0033D^3+0.0822D^2+0.4756D+1.7038$	0.8832
	4	78.9	$\sigma_{ekv} = 5E\text{-}10D^6\text{-}2E\text{-}07D^5+4E\text{-}05D^4-0.003D^3+0.0857D^2+0.3425D+1.9343$	0.8462
15°+15°	1	12.4	$\sigma_{ekv} = 1E\text{-}09D^6\text{-}5E\text{-}07D^5+9E\text{-}05D^4-0.0071D^3+0.2323D^2\text{-}1.9484D+4.5644$	0.704
	2	51	$\sigma_{ekv} = 7E\text{-}10D^6\text{-}3E\text{-}07D^5+4E\text{-}05D^4-0.0025D^3+0.045D^2+0.8656D\text{-}0.1547$	0.8645
	3	60.6	$\sigma_{ekv} = 6E\text{-}10D^6\text{-}2E\text{-}07D^5+3E\text{-}05D^4-0.0017D^3+0.0208D^2+1.1856D\text{-}0.8734$	0.8712
	4	78.9	$\sigma_{ekv} = 8E\text{-}10D^6\text{-}3E\text{-}07D^5+5E\text{-}05D^4-0.0031D^3+0.0604D^2+0.9739D\text{-}0.1622$	0.763
0°+30°	1	12.4	$\sigma_{ekv} = 8E\text{-}10D^6\text{-}4E\text{-}07D^5+8E\text{-}05D^4-0.0059D^3+0.1813D^2\text{-}0.9435D+1.7707$	0.8275
	2	51	$\sigma_{ekv} = 1E\text{-}09D^6\text{-}7E\text{-}07D^5+0.0001D^4-0.0099D^3+0.3281D^2\text{-}2.8843D+6.5965$	0.8627
	3	60.6	$\sigma_{ekv} = 2E\text{-}09D^6\text{-}8E\text{-}07D^5+0.0001D^4-0.0108D^3+0.3579D^2\text{-}3.1909D+6.9559$	0.8572
	4	78.9	$\sigma_{ekv} = 2E\text{-}09D^6\text{-}9E\text{-}07D^5+0.0002D^4-0.0125D^3+0.4166D^2\text{-}3.8895D+7.5362$	0.8501

In Figure 5 and table 3 presents the dependence of the distribution of equivalent stress σ_{ekv} on the von Mises criterion in the mating structural components of the mount disk tool on tetrahedral prism with the destruction of the mountain massif $\sigma comp$. Features of the mountain massif: coal (σ_{comp} = 12.4 MPa; 13.5 MPa; 14.8 MPa) and breed (σ_{comp} = 51 MPa; 60.6 MPa; 78.9 MPa). The analysis of dependencies in the cross section passing through the cutting edge of each of the four disks of diameter D = 160 mm according to the angles of taper: (biconical: $\varphi = \varphi1+\varphi2$= 5°+25° = 30°; 10°+20° = 30°; 15°+15° = 30° and cone φ = 0°+30°).
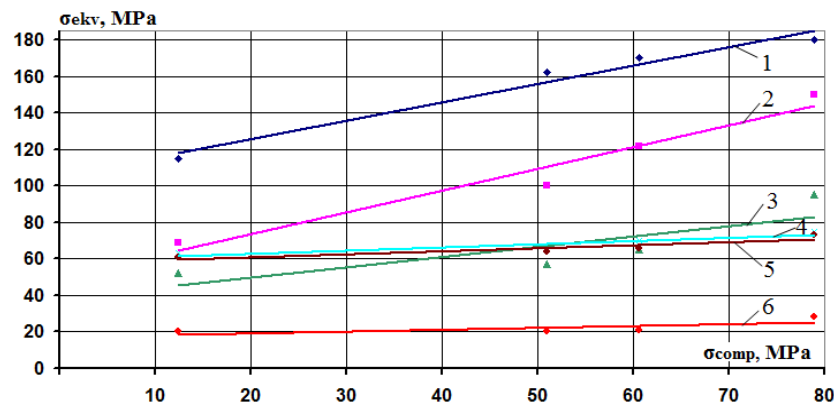
Figure 5. Dependence equivalent stress σ_{ekv} from the tensile strength of the destroyed mountain massif on compression σ_{comp} in diametrical section along the wedge flange of the disk ($\varphi = 5° + 25° = 30°$) for mating structural elements 1–6 (table 3) of the attachment point to tetrahedral prism (Figure 1, d)

Table 3. The distribution of equivalent stresses σ_{ekv} in conjugate constructive elements

of the attachment disk tools to the tetrahedral prisms

Corners sharpening two discs $\varphi = \varphi_1 + \varphi_2,°$		The surface simulation of mating structural elements	Dependence	Validity coefficients of approximation R^2
5°+25°	1	along the edge of the disk	$\sigma_{ekv} = 1.0115\,\sigma_{comp} + 105.44$	0.9711
	2	at the hub of the disc	$\sigma_{ekv} = 1.1923\,\sigma_{comp} + 49.771$	0.9519
	3	on the outer surface of the pivot	$\sigma_{ekv} = 0.5683\,\sigma_{comp} + 38.424$	0.685
	4	on the inner surface of the pivot	$\sigma_{ekv} = 0.1728\,\sigma_{comp} + 59.486$	0.8121
	5	on the outer surface of the axis	$\sigma_{ekv} = 0.1645\,\sigma_{comp} + 57.655$	0.819
	6	in the center of the axis	$\sigma_{ekv} = 0.0997\,\sigma_{comp} + 17.194$	0.5241
10°+20°	1	along the edge of the disk	$\sigma_{ekv} = 1.153\,\sigma_{comp} + 94.515$	0.963
	2	at the hub of the disc	$\sigma_{ekv} = 0.7837\,\sigma_{comp} + 59.495$	0.9911
	3	on the outer surface of the pivot	$\sigma_{ekv} = 0.4563\,\sigma_{comp} + 23.353$	0.9969
	4	on the inner surface of the pivot	$\sigma_{ekv} = 0.273\,\sigma_{comp} + 49.9$	0.851
	5	on the outer surface of the axis	$\sigma_{ekv} = 0.921\,\sigma_{comp} + 35.783$	0.5218
	6	in the center of the axis	$\sigma_{ekv} = 0.2206\,\sigma_{comp} + 22.06$	0.7235
15°+15°	1	along the edge of the disk	$\sigma_{ekv} = 0.9396\,\sigma_{comp} + 103.59$	0.9442
	2	at the hub of the disc	$\sigma_{ekv} = 0.5622\,\sigma_{comp} + 53.984$	0.5191
	3	on the outer surface of the pivot	$\sigma_{ekv} = 0.3284\,\sigma_{comp} + 16.344$	0.9024
	4	on the inner surface of the pivot	$\sigma_{ekv} = 0.1354\,\sigma_{comp} + 56.883$	0.4664
	5	on the outer surface of the axis	$\sigma_{ekv} = 0.5446\,\sigma_{comp} + 47.124$	0.4087
	6	in the center of the axis	$\sigma_{ekv} = 0.3868\,\sigma_{comp} + 9.6287$	0.9629
0°+30°	1	along the edge of the disk	$\sigma_{ekv} = 0.9328\,\sigma_{comp} + 116.43$	0.8789
	2	at the hub of the disc	$\sigma_{ekv} = 0.4487\,\sigma_{comp} + 115.99$	0.9884
	3	on the outer surface of the pivot	$\sigma_{ekv} = 0.4338\,\sigma_{comp} + 38.498$	0.8523
	4	on the inner surface of the pivot	$\sigma_{ekv} = 1.2391\,\sigma_{comp} + 38.897$	0.9435
	5	on the outer surface of the axis	$\sigma_{ekv} = 0.4039\,\sigma_{comp} + 98.013$	0.6492
	6	in the center of the axis	$\sigma_{ekv} = 0.0282\,\sigma_{comp} + 9.5708$	0.9368

3. Displacement in conjugate constructive elements of the attachment of the disk tool to a polygonal prisms

For mating structural elements of the attachment of each of the four disk tools to triangular prisms (Figure 1, a, b, c) and the tetrahedral prisms (Figure 1, d) a simulation of displacement (Figure 6, 7). Results of modeling displacements allow us to estimate the stiffness of the mating structural elements of the attachment disk tool of the instrument including clearances, fits and tolerances, linear and diametrical dimensions in the destruction of face tunneling mining. When modeling the displacement eliminates jamming in the work of the structural elements of the mount, which may occur due to elastic deformations of the structure under load.
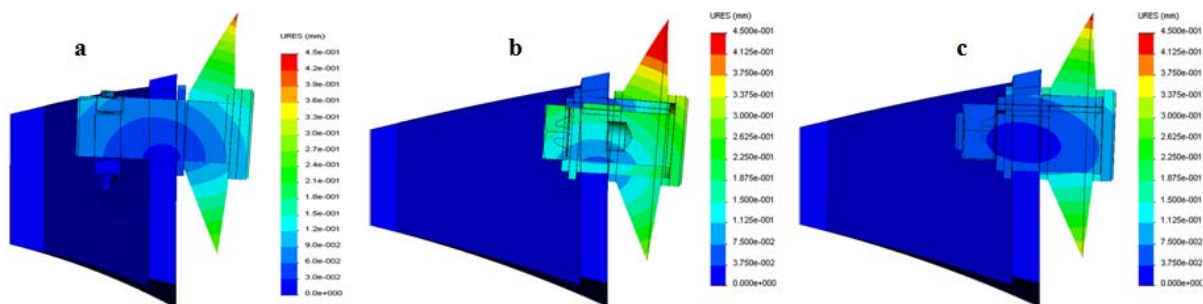

Figure 6. Displacement of structural elements in the attachment biconical disk tool ($\varphi = 5°+25° = 30°$) to the triangular prisms in the destruction of the rock face $\sigma_{comp} = 70$ MPa: a – with strap-lock, b – with screw; c – with nut
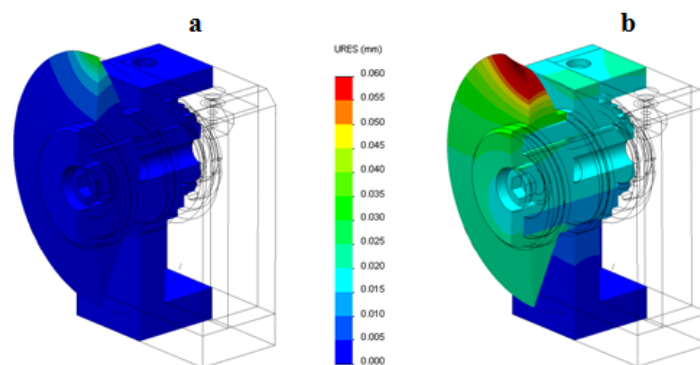

Figure 7. Displacement separate structural elements of the attachment biconical disk tool ($\varphi= 5°+25° = 30°$) to the tetrahedral prisms in the destruction of faces: a – coal $\sigma_{comp} = 12.4$ MPa; b – rock $\sigma_{comp} = 60.6$ MPa

It should be noted that the modeling of the displacements of two separate disk tools with attachment points on tetrahedral prisms in Figure 7 presents through half the image of paintings of the distribution of displacements in the destruction of coal massif (Figure 7, a) and rock massif (Figure 7, b).

Conclusion

The analysis results presented above on the distribution of equivalent stresses σ_{ekv} from conjugate diameters D of the structural elements of the attachment of the disk tool to triangular and tetrahedral prism showed the presence of zones with maximum values in peripheral downhole portion of discs with different angles of taper and the pair of hub discs with the surfaces of pins or axles on which the disc can rotate freely.

The minimum level of equivalent stress σ_{ekv} and displacements in the destruction of faces ($\sigma_{comp} =$ 12.4–78.9 MPa) is marked by the installation of a biconical disk tool ($\varphi= 5°+25° = 30°$; $10°+20° =$

30°; 15°+15° = 30°), a maximum value of equivalent stress σ_{ekv} and displacement was observed when using conical disk tool ($\varphi = 0°+30°$).

In designs biconical disk tool when you change the angles of taper from asymmetric ($\varphi = 5°+25°$; $10°+20°$) to symmetric ($\varphi = 15°+15°$) recorded a reduction in the estimated level of maximum equivalent stress σ_{ekv} and displacements from a symmetric disk for all cases of loading.

Dependence of the distribution of equivalent stresses σ_{ekv} according to the von Mises criterion on the diameter D of the mating structural elements in the cross section passing through the flange of the disk tool on the polygonal prism describes a polynomial dependency of the sixth order. This dependence of the distribution of equivalent stresses σ_{ekv} according to the von Mises criterion on the edges of the disk tools of the console attachment to the tetrahedral prism indicators are destroying the mountain massif σ_{comp} are described by linear dependence.

Marked decrease in the size of zones of maximum equivalent stress σ_{ekv} and displacements on downhole face of the triangular prism (Figure 1, c) drawn to the face in the third variant of the mount disk tool, compared with the second variant (Figure 1, b), which characterizes the increase in the rigidity of fastening of the nut compared to the screw.

The results of these studies allowed the development of a coupled node of the fastening clip of the double disc tool on the tetrahedral prism according to the patent of the Russian Federation 146845 (Figure 1, e). Here, the mating structural elements in the typical section are: disc, pivot, axle with thrust collar. Distinctive features of this technical solution is that the joint condition of free rotation of the two disks represents the coaxial pins-bushings is achieved by the presence of a single prefabricated structural unit, which is made in the form of rigidly attached to each other two axes with thrust ribs, one of which contains a slotted shank, and the other contains a slotted bushing. Such design implies a reduction process jamming and wear double disc tools, rational redistribution of equivalent stress σekv with the notch of the working body of roadheaders with axial crowns.

Recommended combined scheme of the set disk tool on the casing of the distributing gear between axial crowns of the working body of roadheaders with the placement of conical discs in the central zone, and biconical disk in other zones across the width between the crowns.

Further research aimed at modelling and evaluation of stress-strain state of the mating structural elements of the attachment of the coupled disk tools on tetrahedral prisms (patent of the Russian Federation 146845).

References
[1] Aksenov V V, Efremenkov A B, Beglyakov V Yu 2013 The influence of relative distance between ledges on the stress-strain state of the rock at a face *Applied mechanics and materials.* vol. 379, pp. 16-19.

[2] Aksenov V V, Khoreshok A A, Beglyakov V Yu 2013 Justification of creation of an external propulsor for multipurpose shield-type heading machine – Geo-walker *Applied mechanics and materials*. vol. 379, pp. 20-23.

[3] Hong K R, Yang R H 2011 The major problems and countermeasures on the shield machine tunneling in the hard rock stratum *Applied mechanics and materials*. vols. 105-107, pp. 1438-1442.

[4] Prokopenko S A 2014 Multiple service life extension of mining and road machines' cutters *Applied mechanics and materials*. vol. 682, pp. 319-323.

[5] Li X H, Du W, Huang Z L, Fu W L 2011 Simulation of disc cutter loads based on ANSYS/LS-DYNA *Applied mechanics and materials*. vol. 127, pp. 385-389.

[6] Zhao B, Zong X M, He B, Zhang L J 2014 Multi variable multi objective optimization for the cutting head of roadheader *Applied mechanics and materials*. vols. 635-637, pp. 358-364.

[7] Zhang Y, Wang X W, Liu H F 2014 Numerical simulation of rock-breaking process by disc cutter in tunnel boring machine *Applied mechanics and materials*. vol. 487, pp. 513-516.

[8] Li F H, Cai Z X, Kang Y L 2011 A theoretical model for estimating the wear of the disc cutter *Applied mechanics and materials*. vols. 90-93, pp. 2232-2236.

[9] Zhou Z L, Li X B, Zhao G Y, Liu Z X, Xu G J 2011 Excavation of high-stressed hard rock with roadheader *Applied mechanics and materials*. vols. 52-54, pp. 905-908.

[10] Wang X D, Shi M Q, Gao S J, Guo Y C 2014 Design of transverse boom-type roadheader remote control system *Applied mechanics and materials*. vols. 701-702, pp. 679-683.

[11] Khoreshok A A, Mametev L E, Borisov A Yu, Vorobev A V 2015 Finite element models of disk tools with attachment points on triangular prisms *Applied mechanics and materials*. vol. 770. pp. 429-433.

[12] Khoreshok A A, Mametev L E, Borisov A Yu, Vorobev A V 2015 Stress state of disk tool attachment points on tetrahedral prisms between axial bits *Applied mechanics and materials*. vol. 770. pp. 434-438.

[13] Khoreshok A, Mametyev L, Bosirov A, Vorobiev A (2014, October) Stress-deformed state knots fastening of a disk tool on the crowns of roadheaders. *Taishan Academic Forum – Project on mine disaster prevention and control*. Atlantis Press, Amsterdam – Paris - Beijing, pp. 177-183.